Time dependent temperature profile in PC-RAM cell

A PROJECT REPORT

(Submitted in partial fulfilment of the requirements)

submitted by

ASHISH KUMAR TYAGI
EE18M016

for the award of the degree

of

MASTER OF TECHNOLOGY

In

Microelectronics and Photonics

Department of Electrical Engineering
Indian Institute of Technology Madras, India

June 2020

CERTIFICATE

This is to certify that the project entitled **"Time dependent temperature profile in PC-RAM cell"** being submitted to the Indian Institute of Technology, Madras by **Ashish Kumar Tyagi (EE18M016)**, in partial fulfilment of the requirements for the award of the degree of **Master of Technology in Microelectronics and Photonics in Electrical Engineering** is a bonafide record of research work carried out by him under my supervision. The contents of this thesis, in full or in parts, have not been submitted to any other Institute or University for the award of any degree or diploma.

Anbarasu Manivannan
(Project Guide)
Associate Professor
Room Number ESB 332-A
Department of Electrical Engineering
Indian Institute of Technology Madras
Chennai - 600036
INDIA

Place: Chennai
Date:

ACKNOWLEDGEMENTS

One looks back with appreciation to the brilliant teachers, but with gratitude to those who touched our human feelings. The curriculum is so much necessary raw material, but warmth is the vital element for the growing plan and for the soul of the child.

— Carl Jung

I really feel very honoured for having come across brilliant teachers who not only taught me the academic subjects but also touched the deepest chords of my heart. I would like to convey my genuine appreciation and heart-felt gratitude to all of them.

I would like to express my deep sense of gratitude to my guide **Prof. Anbarasu Manivannan** for his guidance, support and encouragement he gave throughout the period of the project work. I am highly

indebted to them for devoting their valuable time. I sincerely thank them for the help and motivation they provided in order to execute this work in good time. Their moral support, unreserved cooperation and generosity, which enabled me to complete the work successfully, will be everlasting in my memory.I owe my sincere acknowledgement to the faculty of the Electrical Engineering Department for their encouragement. They made the best available for Completing the project work. I would like to thank **Dr. Esther Anand,** at Engineering Design Department, IIT Madras for their mentorship and guidance during my MTech project.

I also thank my friends who made my institute life memorable and lab mates who provided constant help when required. Also, words cannot express how grateful I am to my beloved parents for their unconditional support.

Ashish Kumar Tyagi
(EE18M016)

ABSTRACT

Phase change memory is a non-volatile memory technology that utilises the electrical resistivity contrast between resistive amorphous and conductive crystalline phases of phase change materials. These devices operate at high current densities and high temperature gradients which lead to significant thermoelectric effects. I have performed numerical modeling of $Ge_2Sb_2Te_5$ phase change memory cell using COMSOL Multiphysics. Temperature dependent material parameters are used in the model. Strong asymmetry is observed in temperature profiles in all cases: the hottest spot appears closer to the higher potential end suggesting that the thermal profile can be significantly altered by the thermoelectric effects during device operation. Hence, thermoelectric effects need to be considered for device designs for lower power and higher reliability devices.

This paper presents the time dependent temperature profile in Phase change material to find more reliable and fast threshold switching Phase change material for PC-RAM cells.

Two-dimensional finite element simulations of set and reset operation in PCM cells are performed using COMSOL Multiphysics software.

Contents

List of Figures

List of Tables

Chapter 1

Introduction to PC-RAM

The small volume of active media in each memory cell acts as a fast programmable resistor. PCM devices are programmed by electrically altering the structure (amorphous or crystalline) of a small volume of chalcogenide alloy. The programming pulses drives the memory cell into a high or low resistance state (pulse transition process), depending on current magnitude. Phase transition process can be completed in as quickly as 5 nanoseconds. Information stored in the cell is read out by measurement of the cell's resistance.

Phase change memory (PCM) has become a technology of interest for non-volatile memory over the past 15 years. The concept of PCM originated in the 1960s, however it only recently has been considered

viable for storage class memory due to the improvements in fabrication technology and materials engineering.

1.1 Device operations

There is a need for a next-generation NVM that might have an easier scaling path than NAND flash to reach the higher densities offered by future technology nodes. Fortunately, new NVM candidate technologies have been under consideration as possible Flash "replacements" for more than a decade. Each of these (PCM, ReRAM and solid-electrolyte memory) has its strengths and weaknesses.

Fig 1.1(a) shows Phase change materials (PCMs) such as chalcogenides like $Ge_2Sb_2Te_5$ (GST) have amorphous(a) and crystalline(c) phases with contrasting electrical and optical properties.

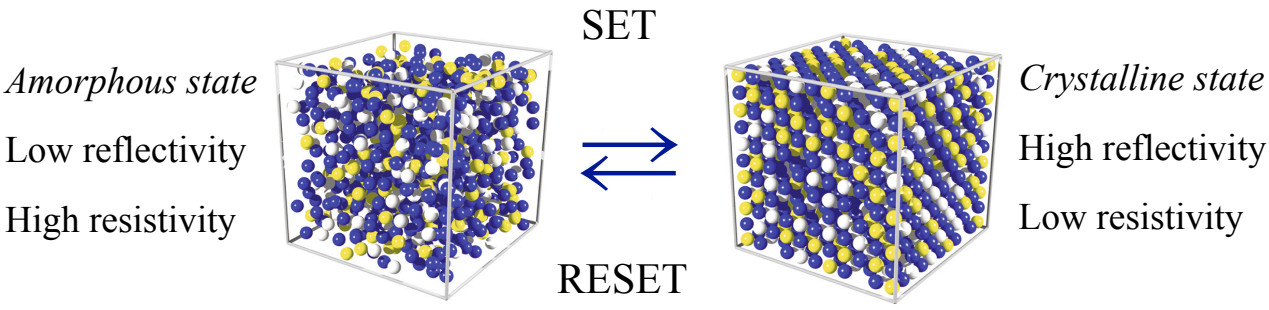

Fig. 1.1(a) GST Phase-transition

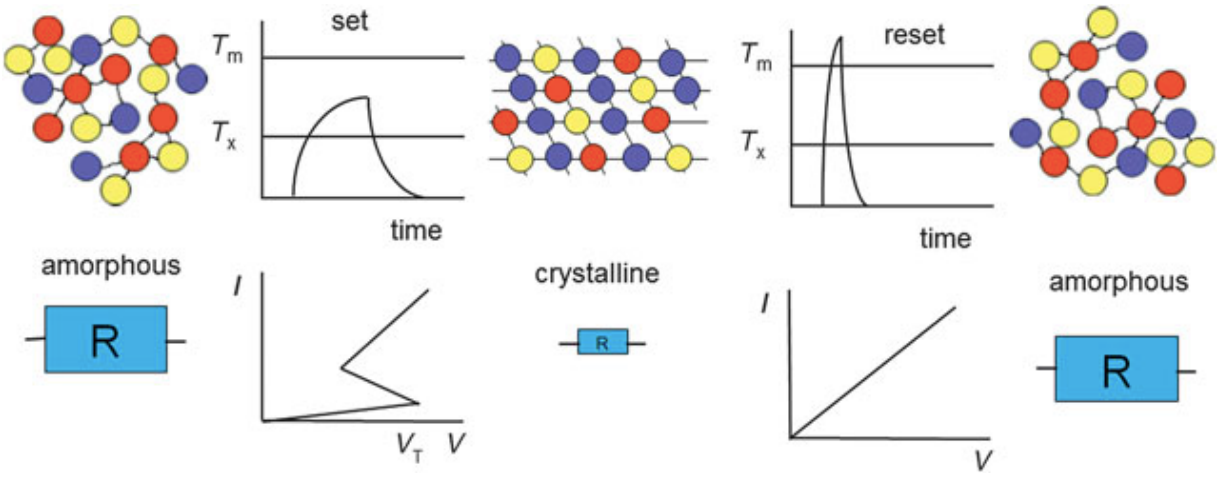

Fig. 1.1(b) PCM Characteristics

Fig 1.1(b) shows the large resistivity contrast between crystalline (low resistivity) and amorphous (high resistivity) phases of the phase change materials. Set and Reset state of PCM refers to low and high-resistance state, respectively.

As fabricated, the phase change material is in crystalline, low-resistance state because the processing temperature of the (BEOL) metal interconnect layers is sufficient to crystallise the phase change material. GeSbTe has two state states, crystalline and amorphous. The phase change mechanism from high resistance amorphous phase to low resistance crystalline phase in nano-timescale and threshold switching are two of the most important characteristic of GeSbTe.

Fig 1.2(c) shows one common PCM cell. To reset the PCM cell into the amorphous state, the programming region is first melted and then quenched rapidly by applying a large electrical current pulse for a short time period. Doing so leaves a region of amorphous, highly resistive material in the PCM cell. This amorphous region is in series with any crystalline region of the PCM and effectively determines the resistance of the PCM cell between the top electrode contact (TEC) and the bottom electrode contact (BEC). To set the PCM cell into the crystalline phase, a medium electrical current pulse is applied to anneal the programming region at a temperature between the crystallization temperature and melting temperature for a time period

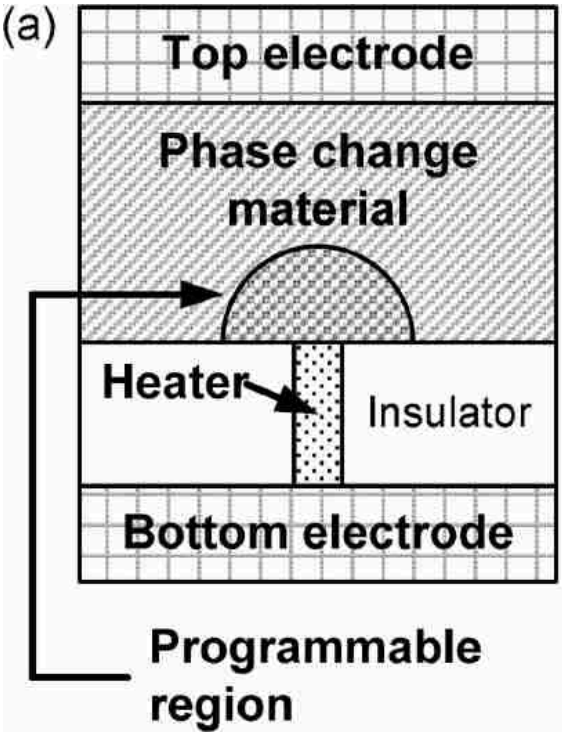

Fig. 1.2(a) PCM cell

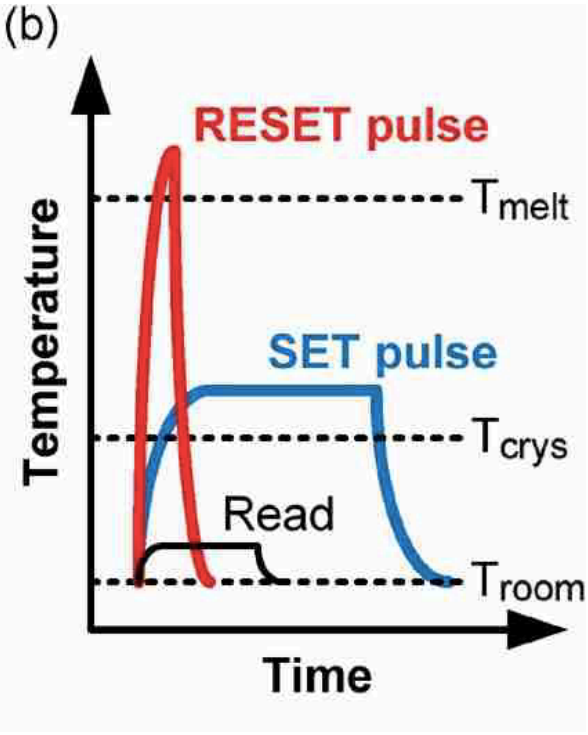

Fig.1.2(b) Pulse shapes

Long enough to crystallise. To read the state of the programming region, the resistance of the cell is measured by passing an electrical current small enough not to disturb the current state(roughly 20% of set pulse). The schematic pulse shapes re summarised in Fig. 1.2(b)

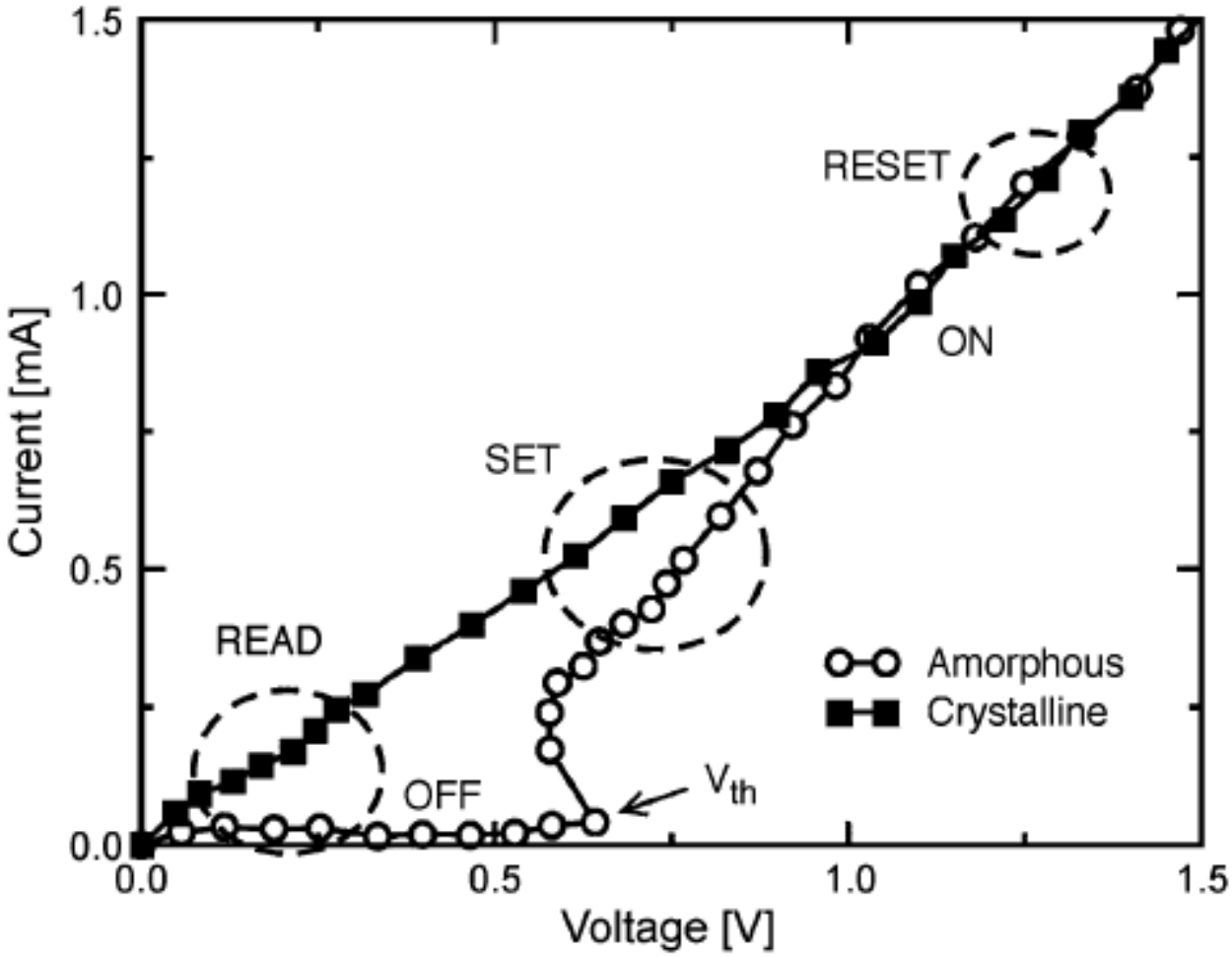

Fig. 1.2(c) I-V characteristic of set and reset state

Fig. 1.2(c) shows current-voltage(I-V) curves of the set and reset states. The set and reset states have large resistance contrast for voltages below the threshold switching voltage (Vth).

The reset state is in the high-resistance state below Vth (subthreshold region) and shows electronic threshold switching behavior at Vth, i.e., a negative differential resistance. This is reversible if the voltage pulse is removed very quickly. But if the voltage is applied for longer than the crystallization time it leads to memory switching and the cell reaches the low-resistance state for an applied voltage larger than Vth. The set process critically depends on the above mentioned electronic threshold switching effect. When the electric field across the amorphous region reaches a threshold value, the resistance of the amorphous region goes into a lower resistance state which has resistivity that is comparable to the crystalline state.

This electronic threshold switching phenomenon, the physics of which is yet to be fully explored, is the key to successful set programming of the PCM. When the PCM is in the reset state, the resistance of the PCM cell is too high to conduct enough current to provide Joule heating to crystallize the PCM cell. The electronic threshold switching effect lowers the resistance of the phase change material to the dynamic resistance and enables set programming.

1.2 Motivation

PCM is a resistive memory technology, where a '1' or '0' is represented by a low-resistance state or high-resistance state in the device. Billions of write and erase cycles are achieved by using a chalcogenide glass such as Ge2Sb2Te5 (GST) which can repeatedly and rapidly change phase between crystalline (low-resistance) and amorphous (high-resistance) states[17]. Changing the material from crystalline to amorphous state (reset) requires melting and rapid freezing of a small volume of the material such that the atoms do not have time to arrange in a crystalline fashion. Reversing the phase back to crystalline state from amorphous state (set) requires heating the material above its crystallisation temperature for a sufficient time so that the atoms rearrange themselves in crystalline order (Figure 1.2(b). The timescale for a reset operation is in the order of ~ 10 ns, and is in the order of ~ 100 ns for a set operation. PCM shows promising results for device scaling into the nanometer scale as reduced dimensions result in lower power and current requirements, as well as higher packing density and higher speed of operation [18].There is considerable interest in studying and modeling phase

transitions and device operation in GST PCM cells for the development of PCM technology [17] [18], as there are three phase transitions that take place (amorphous to crystalline, crystalline to liquid, and liquid to amorphous). The importance of using temperature dependent material parameters in the finite element modeling of a reset operation is demonstrated, capturing the non-linear current-time (and thus temperature-time) characteristics that occur during the crystalline to liquid phase transition and show the impact of the non-linear behavior for various load conditions and geometries. However, the amorphous to crystalline phase transition is of the most interest as it is has additional complexity in the phenomena of nucleation and growth of crystal grains and it is important for understanding the set operation as well as fabrication processing techniques. Simulations performed in COMSOL Multiphysics enable this crystallization model to be compatible alongside any other physics such as joule heating and solid mechanics. This approach allows for the modeling of crystallization during a set/reset operation or a fabrication process step, allowing for material properties to be dynamically updated and applied to areas that are constantly changing shape in the simulation, which can be

otherwise be very difficult in a finite element model with static domains.

1.3 State Of The Work: Literature Review

This section provides a comprehensive review of the literature to the phase change random access memory. Emphasis is given to both historical papers of classical importance, as well as to the current state of the art.

Many literatures exist in the academic world regarding the design of PC-RAM Cell. There are a number of time varying properties of GST materials to examine when heating. The PCM was fabricated with 45 nm technology and consists of an active $Ge_2Sb_2Te_5$ (GST) layer between a confined bottom electrode (or heater) and a top electrode (Servalli, 2009). The PCM top electrode was made of a Cu/W/TiN multilayer connecting all cells along a row in the array, while the bottom electrode consisted of a tungsten plug and a sublithograpic TiN heater connected to the GST layer.(lelmini and Zhang, 2007).

In 1969, Sie demonstrated a prototype of a PCM device by integrating chalcogenide film with a diode array [3, 4]. In 1970, Neale, Nelson,

and Moore (later known as the cofounder of Intel) demonstrated the world's first 256−bit PCM [5].

PCM is the top contender for the future of nonvolatile memory, preceded by more than 45 years of investigation. The primary products/applications, which PCM will impact, are memory-type or storage-type SCM [8], [9] and Embedded memory[10].

The logical state of the phase-change memory cell described by Lankhorst et al[7]. The thermal properties of the cell in the report by Sebastian et al. Wei Zhang, Riccardo Mazzarello, Matthias Wuttig and Evan Ma presented the paper which was mainly concerned the role of crystallisation in enabling neuro-inspired computing using PCMs. To make a universal memory device, fast switching speed is important. The insufficient switching speed of commercialised GST- based PRAMs is limited by the stochasticity of nucleation. In a conventional memory cell (150 nm- thick and in contact with a 190 nm- diameter bottom electrode the minimum SET time is >10 ns.

A wide variety of materials have been developed, which aim at improving the desired phase-change properties. The most-promising areas are doped GeSbTe[11], new materials with composition

deviations from GeSbTe, ALD- or physical vapor deposition (PVD)-based materials, and finally superlattice phase-change materials[12].

1.4 Limitations

Most relevant to the operation of PCM are the structural physical properties which affect the temperature profile (how much heat is generated and where), the critical limiting cross-sectional aperture (which must be fully blocked to get high resistance/reflectivity contrast), and the volume where the phase change material undergoes repeated melting and crystallisation. Crucial features of the cell are the aperture size and shape, the thickness and uniformity of the phase change material, the resistivity and interface resistance of electrodes, the thermal conductivities of surrounding materials, and the stresses on the active switching volume introduced by surrounding material.

Overall, PCM memories are promising NVM, because they offer simultaneously low read/ write latency, high throughput performance, and high endurance while being highly scalable[13-16]. Nevertheless, a number of issues remain critical, which makes the transition towards a large integration density difficult. The power consumption, or more

precisely the high current needed for the RESET operation, the data retention, that is linked to the cell's ability to avoid unintended recrystallisation, and resistance drift after programming, which corresponds to a significant increase of the resistance value of the amorphous phase with time have been the most challenging issues so far.

1.4 Objectives

The primary goal of this project is to model, design, control and implement a phase change memory cell. In simple terms, the project aim is to a 2D/3D simulation for PCM material to find a more reliable and fast threshold switching material and design.

To achieve these goals and to broaden my understanding of the subject, the following milestones will have to be reached.

- Heat transfer model and source equation
- Design a cell structure and implement laser heating
- Select material properties for GST and other components
- Design and implementation of 3D/2D simulation

- Time dependent temperature profile for PC material
- Generating SET and REST pulses and by using RF and AC/DC model under COMSOL Multiphysics Software version 5.2.
- Compare Simulated and Experimental results.

Chapter 2

Theoretical modeling

2.1 Nanosecond laser pulse generation

In this chapter, a theoretical thermal model based on a stationary pulsed, ns-laser beam interaction with GST based PCM cell is explained. Influence of the laser fluency and the influence of laser beam profiles such as Gaussian and line beam on the crystalline characteristics and phase change is also investigated.

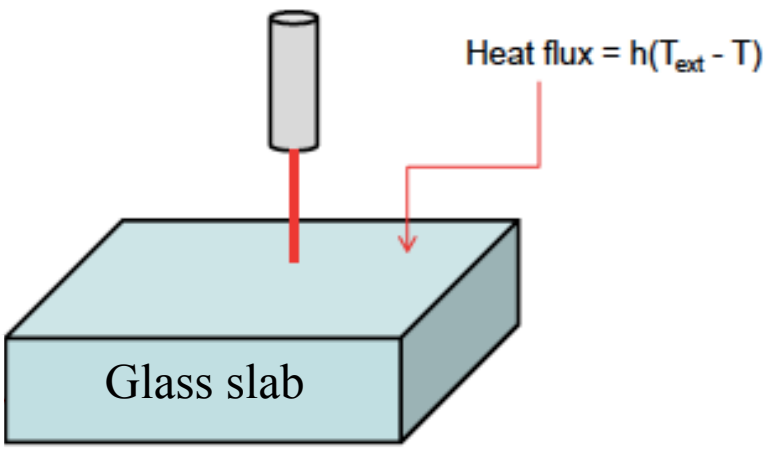

Fig.2.1(a) Model definition for laser source

The effect of the complex reflective index of glass is modelled using absorption and reflection coefficient. Here the modelling geometry only includes the glass slab. The heat flux on the top surface simulates convective cooling. The estimated heat loss by convection (hconv) and radiation (hrad) is given as follow:

$$h_{conv} = h\,(T_s - T_a) = 70.8 \times 10^3 \text{ W/m} \quad (2.1)$$

$$h_{rad} = \varepsilon\sigma\,(T_s^4 - T_a^4) = 6.05 \times 10^3 \text{ W/m} \quad (2.2)$$

In equation 2.1 and 2.2, assuming that assuming that ε = 0.46 (emissivity of a material) [17], h = 177 (Heat transfer coefficient) [18], σ = 5.67 x 10^-8 W/m^2K^4 (Stefan Boltzmann constant), T_s = 700K (Maximum surface temperature), T_a = 300 K (ambient temperature). The energy loss due to the Planck radiation and heat convection to the surroundings is very small in comparison with the laser beam energy. Hence convective and radiative losses are negligible ($I_{loss} < 10^{-6} I_0$).

A three dimensional and two dimensional heat transfer models are used for estimating the the film temperature profile at 250 nm laser wavelength. This theoretical simulation is used to identify the threshold switching and crystallisation of GST225.

Calculating the heat input

The absorbed energy along the depth depends on the exponential decrease in the intensity as per the *Beer-Lambert's law*. The source term is given by the following equation:

$$Q(x,y,z) = \mathrm{Q}_0(1-\mathrm{R}_c)\frac{A_c}{\pi\sigma_x\sigma_y} e^{-\left[\frac{(x-x_0)^2}{2\sigma_x^2}+\frac{(y-y_0)^2}{2\sigma_y^2}\right]} .e^{-A_c z} \qquad 2.3$$

Q_0 total power input, include the time dependence, $\exp(\frac{t-t_0}{t_{pulse}})^2$ factor. R is the reflective coefficient, Ac is the absorption coefficient, first exponential term is 2D gaussian distribution in xy plane, second one is exponential decay due to absorption. Thus the source equation refers to the incident laser pulse with gaussian temporal profile. The spatial profile was assumed to be either with a Gaussian or with a flat-top intensity distribution. Same source equation can be modified for 2D Heat Transfer model.

$$Q = Q_0 \cdot (1 - R_C) \cdot \frac{A_C}{\pi \cdot \sigma_x} e^{-\frac{x^2}{2\sigma_x^2}} \cdot e^{-A_C \cdot y} \qquad 2.4$$

The wavelength dependent absorption coefficient Ac and the reflectivity R (65%) of the material are incorporated in the source equation and t_{pulse} represents half the pulse width, which corresponds to full width at half maximum (FWHM). And for the flat-top beam profile, $I_0(x)$ was considered uniform ie., $I_0(x) = I_0$.

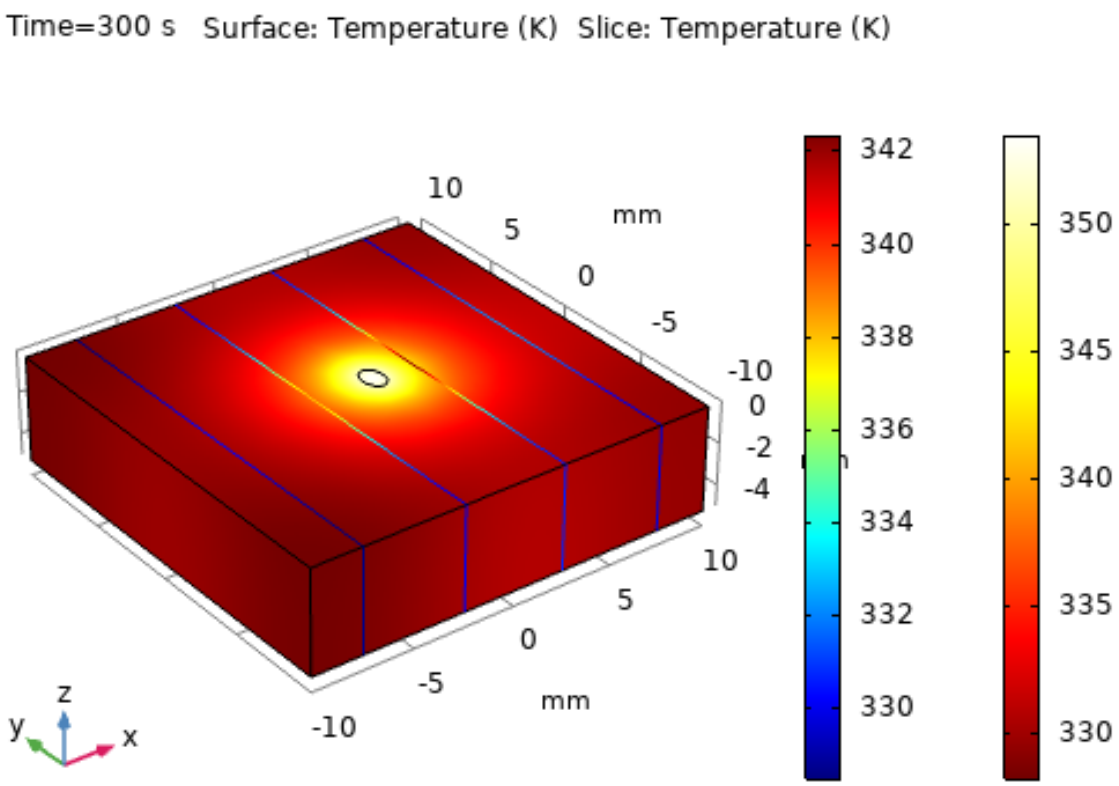

Fig. 2.1(b) shows the temperature profile in glass slab with four slices

This elliptical surface created on the top surface is used to guide a finer mash in the area where the laser beam is incident upon.

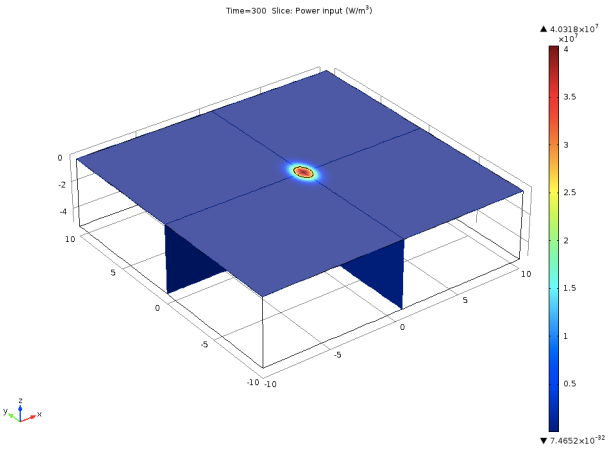

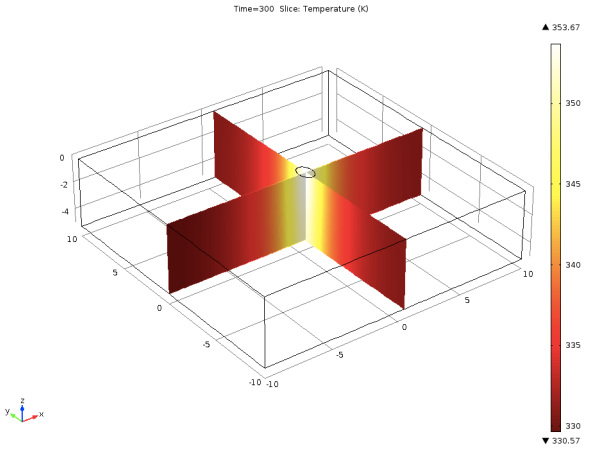

Fig. 2.1(c) Slice plots of heat input Fig.2.1(d) Slice plots of temperature

Fig. 2.1(c) and (d) shows the temperature distribution at surface and within glass, with the help of slices. The top surface is aligned with z = 0. Hence the effect of absorption can be simulated by the term exp(-Ac*abs(z)). The centre of the beam can be easily shifted by changing x_0 and y_0. The beam width and astigmatism can be easily controlled by the standard deviation parameters: sigma(x) and sigma(y). Slab size L 20 mm and slab thickness Lz 8 mm pulse centre coordinate (0.5mm, 0mm) and pulse standard deviations (0.5mm, 0.75mm) are used.

The cell temperature within a nanoscale PCM device during the set operation is using the modelling of thermal transport. We can calculate power dissipated on the cell using voltage and current during the set pulse. This heat transfer method can be used with RF

and DC models to characterise the time dependent temperature-dependent crystallisation process within a PCM-cell.

2.2 Material Parameters

Some of the major physical properties of Ge2Sb2Te5 and TiN and others are tabulated in Table 1.

Table 1

Properties	Ge2Sb2Te5	TiN	SiO2
Melting point, °K	700	1640	
Mass Density, g cm^{-3}	5.5	5.43	2.18
Thermal conductivity K, W m^{-1} K^{-1}	$K_{GST}(T)$(Ref. 19)	$K_{TiN}(T)$ (Ref. 21)	1.38
Electrical conductivity, σ (Ω–1·m–1)	$\sigma_{GST}(T)$(Ref. 19)	1×10^6–1×10^7	
Specific heat, C_p (J/kg/K)	202	784(Ref.21)	703
electron-photon coupling strength γ	10^17 W/(m3·K)		
Activation energy ($\Delta\xi_{am}$)	0.32 eV		
Activation energy ($\Delta\xi_{cryst}$)	0.04 eV		1.65 eV, 500°C
Electrical Permittivity (Epsilon)	11.7	0.315	
absorption coefficient (Ac)	0.08 nm^-1	0.28863	

Table 1 Major physical properties of GST225, TiN and SiO2.

2.3 Simulation

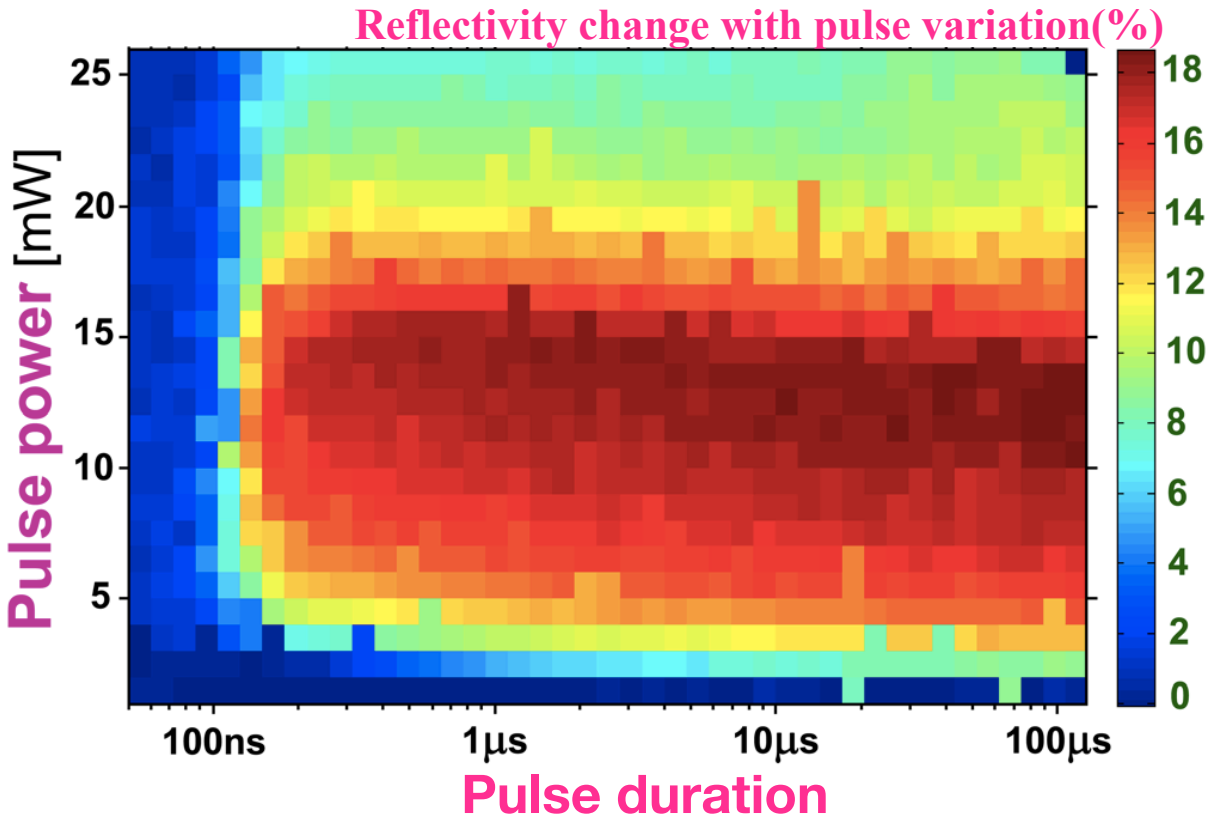

Fig. 2.2(a) Optically-induced reflectivity change (normalised) of a standard GST225 sample as a function of laser-pulse duration and power. As expected, rapid crystallisation occurs at moderate powers for pulses as short as 100 ns.

Theoretical simulation was performed using the COMSOL Multiphysics (version 5.2) and temperature profiles along the depth direction of the irradiating spot on the GST film were investigated. Figure 2.2(a) shows the reflectivity change (normalised) of our $Ge_2Sb_2Te_5$ sample as a function of laser power from 1 to 25 mW, and

of pulse duration from 50 ns to 100 microseconds. This measurement corresponds to the first crystallisation of our GST225 sample, which is nucleation-dominated material.

This rapid speed of crystallisation (100 ns) is one of the features that made $Ge_2Sb_2Te_5$ such an attractive material for both optical and non-volatile phase change memory applications.

Fig. 2.2(b) shows the temperature profile in GST225 after 20 ns single pulse irradiation with a fluency of 15 mJ/cm^2. It is observed that the GST film on Si[100] substrate is characterised by a uniform temperature field upto thickness of about 80 nm which is corresponds to the film thickness in this study.

Consequently, it is assumed that also for higher laser fluences the complete films can be described by a defined temperature. At these low laser fluences, the temperature increases by about 30K only.

Higher temperature rises can be expected for higher laser fluences. The phase transformation processes are generated by irradiation with 20ns laser pulses at a wavelength of 250 nm and are investigated in dependence on the number of pulses and the laser fluence.

A reversible phase transition is realized by using pulse numbers will be transition is realized by using pulse numbers are equal to or less then 5 at fluences above the threshold fluence between 11 and 15 mJ/ cm^2 for crystallization and single pulses at a fluence between 166 and 182 mJ/cm2 for amorphization.

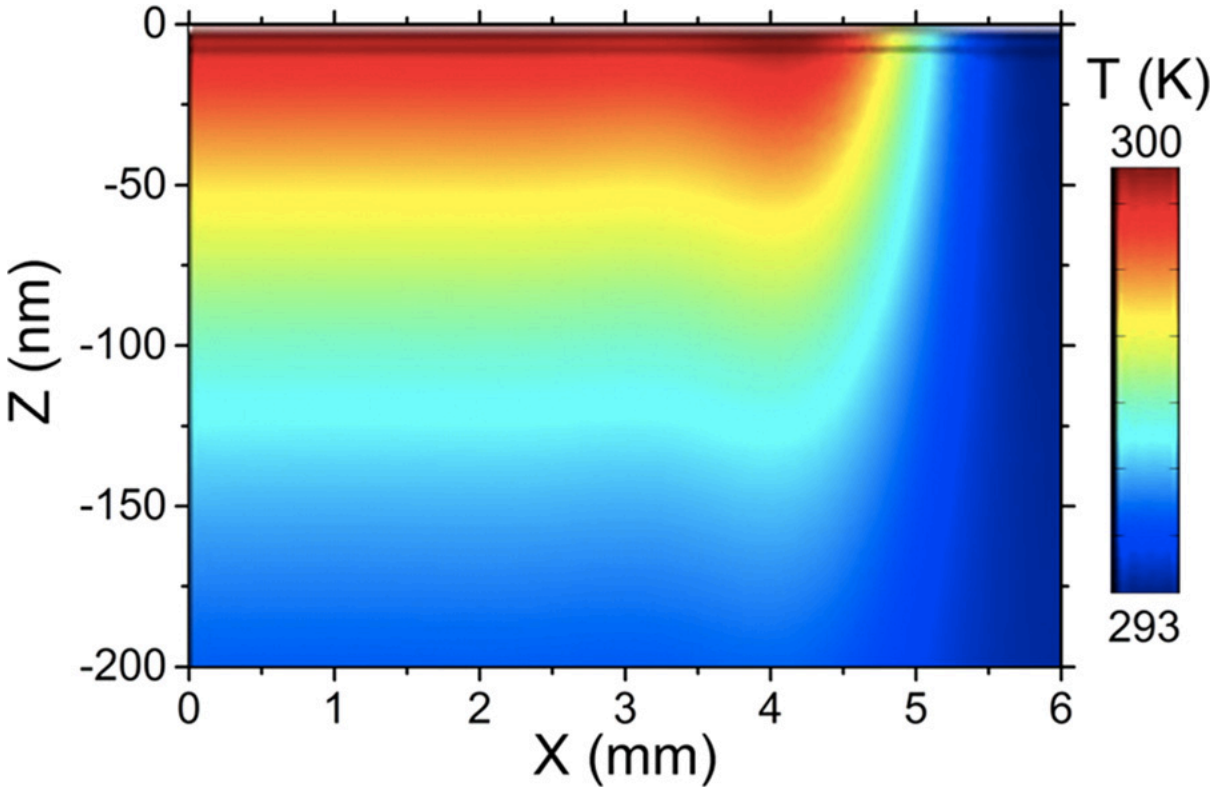

Fig. 2.2(b) 2D temperature distribution of a 80 nm thick GST225 film on Si[100] substrate after single laser pulse irradiation with a fluence of 15 mJ/cm^2 for 20 ns. z is the depth, x is the distance from the laser spot center.

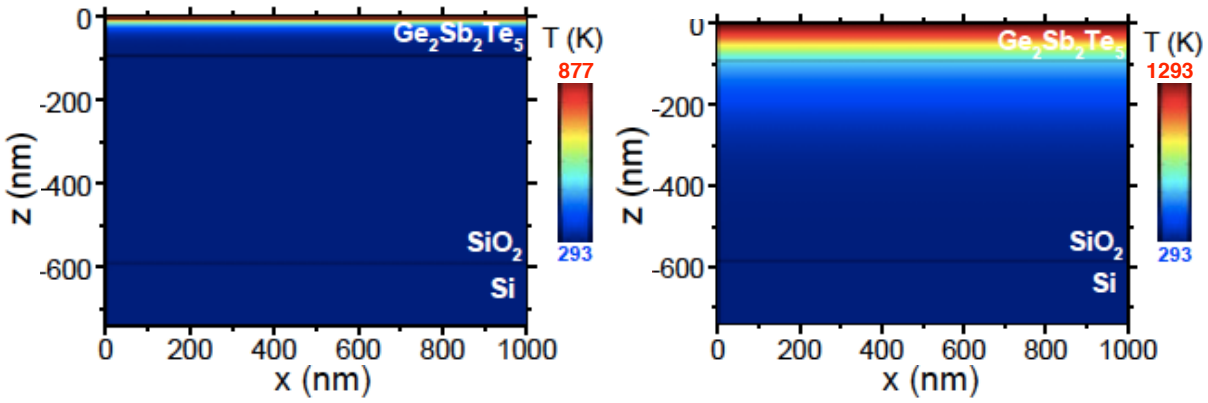

Fig. 2.2(c) Fig. 2.2(d)

Fig. 2.2(c) and (d) 2D temperature distribution of a 80 nm thick GST film on a SiO2/Si substrate: (c) after single fs pulse laser irradiation with a fluence of 20 mJ/cm2 for 50 ps, (d) after single ns pulse laser irradiation with a fluence of 36 mJ/cm2 for 20 ns. z is the depth, x is the distance from the laser spot center.

Figure 2.2(c) shows the two-dimensional temperature distribution in a 80 nm GST and 500 nm SiO2/Si substrate system 50 ps after the single pulse femtosecond laser irradiation with a fluence of 20 mJ/ cm^2, as compare to ns one (see in Fig. 2.2(d)). The temperature distribution after fs pulse laser irradiation shows a surface-localised heating region, where there is a relatively fast temperature rise and a higher temperature in the top surface of the GST film with a larger temperature gradient through the layer thickness.

The material parameter of SiO2 and Si was taken from the COMSOL material data base. At this first estimation the material (GST225) parameter are assumed as constant. This model is for an estimation of the maximum achievable temperature induced by the laser radiation. Further energy loss mechanism like laser-plasma absorption and melting and evaporation enthalpy were non-regarded. Although the surface temperature increases by about 877 K in the top surface, which is much higher than the conventional crystallisation temperature (~ 750°K) for GST film, the crystallisation temperature.

The aim of the model is an estimation of the maximum achievable temperature induced by the laser radiation. For fs laser irradiation are describing the non-equilibrium process, which is more accurate used than normal thermal diffusion equations. During laser-material interaction, the electrons in the materials are first excited by the deposited laser energy and these “hot” electrons are then cooled by transferring their energy to the lattice through electron-phonon coupling.

Chapter 3

Simulation of Set and Reset Operations

3.1 Modeling

A physical-realistic model is required to provide insight into temporally and spatially resolved kinetics of writing current, device temperature, and phase transition for the required amorphized process. Includes several equations, comprising the Laplace equation and the heat transfer equation to compute temperature and cooling rate inside the Chalcogenide Ge2Sb2Te5 layer, given by

$$\nabla \cdot J = -\nabla \cdot (\sigma(T,E)\nabla V) = 0 \tag{3.1}$$

$$d_{\mathrm{GST}} \cdot C_P(T)\frac{dT}{dt} - \nabla \cdot (\kappa(T)\nabla T) = \frac{J \cdot J}{\sigma(T,E)} \tag{3.2}$$

where σ is the electrical conductivity; V is the electric potential; ρ is the density; Cp is the specific heat; T is the temperature; k is the thermal conductivity; E is the electric field.

COMSOL 3-D finite element simulations of joule heating in PCM cell are performed by coupling Heat Transfer by Conduction and Conductive Media DC physics modules. The heat transfer model includes heat diffusion and joule heating. The current continuity model includes only the drift term.

The total conductivity of a-GST is modeled as the combination of the electrical breakdown component [$\sigma_E(E)$] and the temperature-dependent conductivity [$\sigma_T(T)$] such that $\sigma(T,E) = \sigma_T(T) + \sigma_E(E)$. $\sigma_E(E)$ is assumed to be an exponential function amounting to 1% of the room-temperature conductivity of a-GST at zero field and 10% of the molten conductivity of GST at breakdown.

$$\sigma_E(E) = 0.0364 \cdot e^{\left(|E| \cdot 239.5 \times 10^{-9}\right)} (S/m). \qquad 3.3$$

This assumption enables the use of field to approximate electrical breakdown, which is responsible for self heating of a-GST. The contributions of vertical (Ez) and radial field (E_r) dependent

components were added separately [$\sigma_E(E) \approx \sigma_E(E_z) + \sigma_E(E_r)$] to minimize the simulation complexity. The error introduced by this simplification is expected to be insignificant due to relatively small contribution of E_r. Field dependence is neglected for c-GST since electric field is small due to high conductivity, $\sigma_T(T)$ is very larger to compare with $\sigma_E(E)$. The current continuity (3.1) and heat transport (3.2) equations are solved self-consistently in COMSOL Multiphysics.

3.2 Simulation setup

COMSOL Multiphysics 5.2 is used to simulate the phase- change of cell using a finite element, 3-D physical model for PCM cell coupled with a SPICE model for R_L, C, and V_{pulse} to explore the effects of scaling device length, capacitance, load resistance, and supply voltage (Figure 3.1(a)). Temperature dependent electrical resistivity (ρ) and thermal conductivity (κ) for GST225 are used in the simulations.

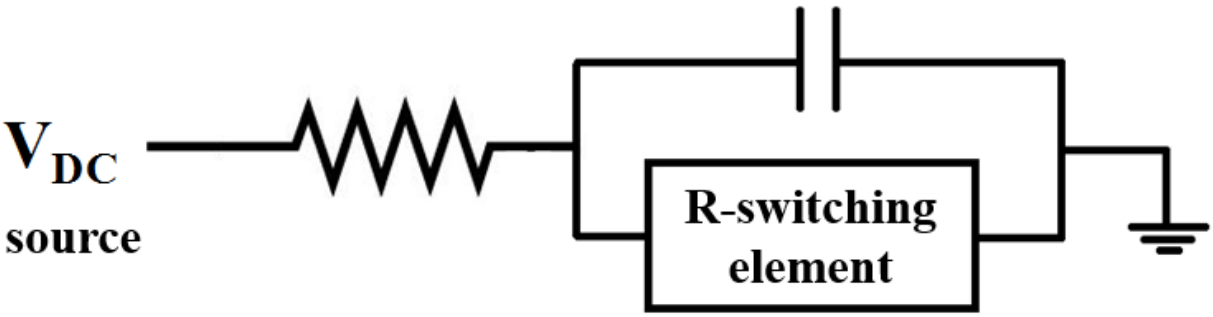

Fig. 3.1 Circuit schematic of DC model comprised of a DC voltage source, a resistor, and a capacitor in parallel with a resistance switching element.

The 3-D model of the wire is inserted into a SPICE simulation as a resistive element along with the DC supply, RL and C (figure 3(b)). The SPICE model and the 3-D finite element model are solved self-consistently to capture the circuit response to any temperature change in the GST and vice-versa.

The Laplace equation is solved to provide the electric field and current density distributions inside the GST layer, which are simultaneously implemented as the heat source for the heat transfer equation, performing the calculations of temperature and cooling rate distributions inside the GST layer. In our simulation, the crystalline GST turned into its amorphous state in the region where the temperature exceeded the melting point (i.e., 620°C) , and the cooling rate was greater than 37°C/ns. In this case, the electrical

conductivity of the Ge2Sb2Te5 alloy was defined by:

$$\sigma_{GST} = \sigma_{am} \cdot (T >= 620\ °C) \cdot (Tt \geq 37\ °C/ns) + \sigma_{cryst} \cdot ((T < 620\ °C) \| (Tt < 37\ °C/ns)) \quad 3.3$$

where Tt is the cooling rate, and σ_{am} and σ_{cryst} are the electrical conductivity of the Ge2Sb2Te5 alloy in its amorphous and crystalline phases respectively, given by (3.4) :

$$\sigma_{am} = \sigma_{0am} \times \exp(-\Delta\xi_{am}/k_B T) \times \exp(E/E_0) \quad 3.4$$

$$\sigma_{cryst} = \sigma_{0cryst} \times \exp(-\Delta\xi_{cryst}/k_B T)$$

where σ_{0am} and σ_{0cryst} are prefactors for amorphization and crystallization with a value of 1.88× 10^4 Ω−1·m−1 and 1.5 × 10^4 Ω−1·m−1, respectively; $\Delta\xi_{am}$ and $\Delta\xi_{cryst}$ are the activation energies for the temperature dependence of amorphous σ_{GST} and crystalline σ_{GST} with a value of 0.32 eV and 0.04 eV, respectively; E_0 is the critical electric field with a value of 5 × 10^7 V·m−1. The thermal conductivity of PC materials is important because it strongly influences the thermal response of a PCM device to an electrical current pulse. The thermal conductivity of the Ge2Sb2Te5 alloy is described in a similar manner to its electrical conductivity, given by:

$$k_{GST} = k_{am} \cdot (T >= 620\ °C) \cdot (Tt <= -37\ °C/ns) + k_{cryst} \cdot ((T < 620\ °C) \| (Tt > -37\ °C/ns)) \quad 3.5$$

where k_{am} and k_{cryst} are the thermal conductivities of amorphous and crystalline Ge2Sb2Te5 with a value of 0.2 W·m−1·K−1 and 0.58 W·m−1·K−1, respectively.

3.3 Simulation

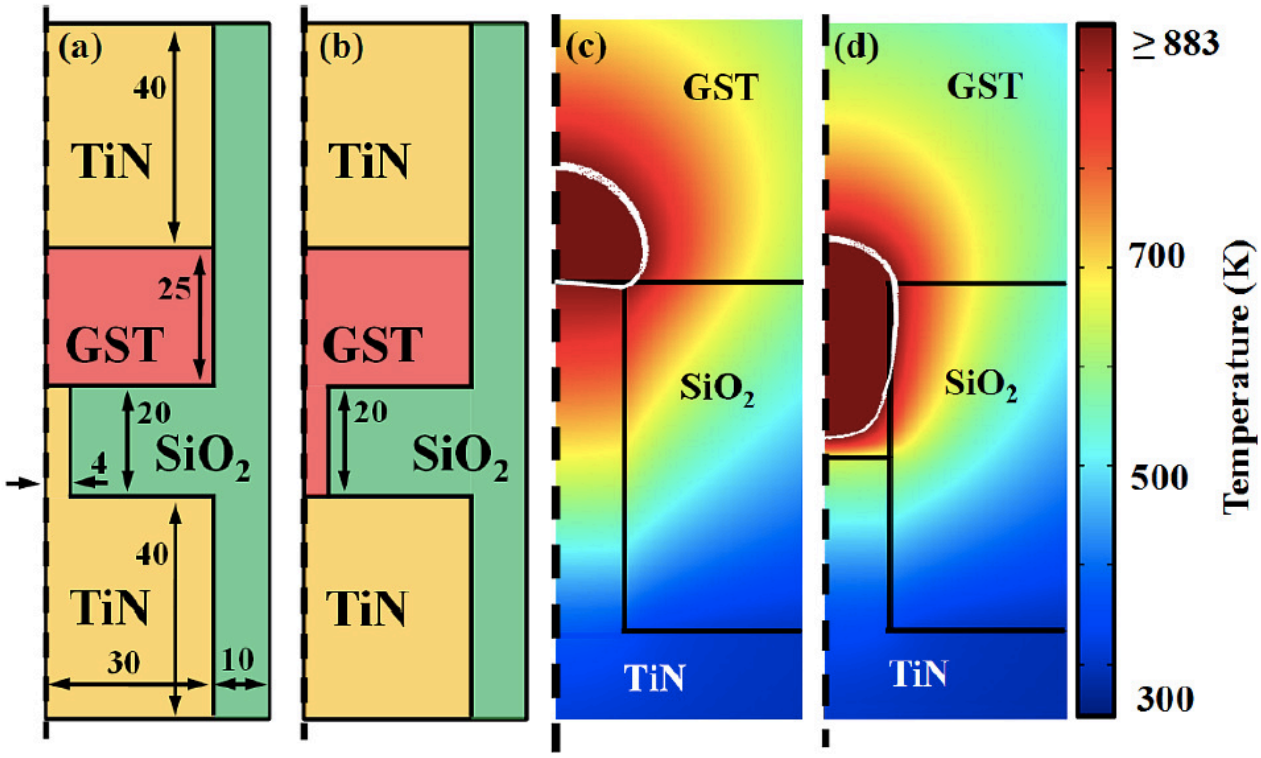

Fig. 3.2 (a) Schematics of a conventional planar mushroom cell design with an extension of the Ge2Sb2Te5 (GST) active region with dimensions marked in nm, and (b) a confined cell with 20 nm GST extension length. (c) Peak thermal profile of a planar mushroom cell with 25 nm film thickness during reset pulse (biased with 0.83 V) compared to (d) a confined cell with 25 nm film thickness and 10 nm GST extension length (biased with 0.76 V). Dotted lines mark the axis of rotational symmetry in each case, and a white contour line denotes the boundaries of melting in the active region.

Two-dimensional finite element simulations of reset operation in PCM cells are performed using COMSOL Multiphysics software to predict how variations in geometry and load resistance affect device performance.

In particular, we examine the confined cell, similar to the well-known mushroom cell design except that the phase change material is extended into the confined pillar (Figure 3.2(b)). In our simulations we incrementally recess the bottom contact, extending the active region into the confined heater and compare a range of confined cell geometries. [Fig. 3.2(c),(d) and 3.5] are simulated using the half-device geometries shown in Fig. 3.2(a)–(b) with rotational symmetry around the left side and 1-kΩ series resistor, and C = 15-20 fF.

The latent heat of fusion (Lf = 126 x 10^3 J/kg) is incorporated as a spike in heat capacity (CP) at the melting temperature, as illustrated in the inset of Figure 3.2(a). Mass density(d) of GST is modeled as a constant at 6200 kg/m3. Temperature dependent σ and κ are also used for TiN, as shown in Figure 3.3(b). CP and mass density of TiN are modeled as constants of 784 J/kg.K and 5430 kg/m^3, respectively.

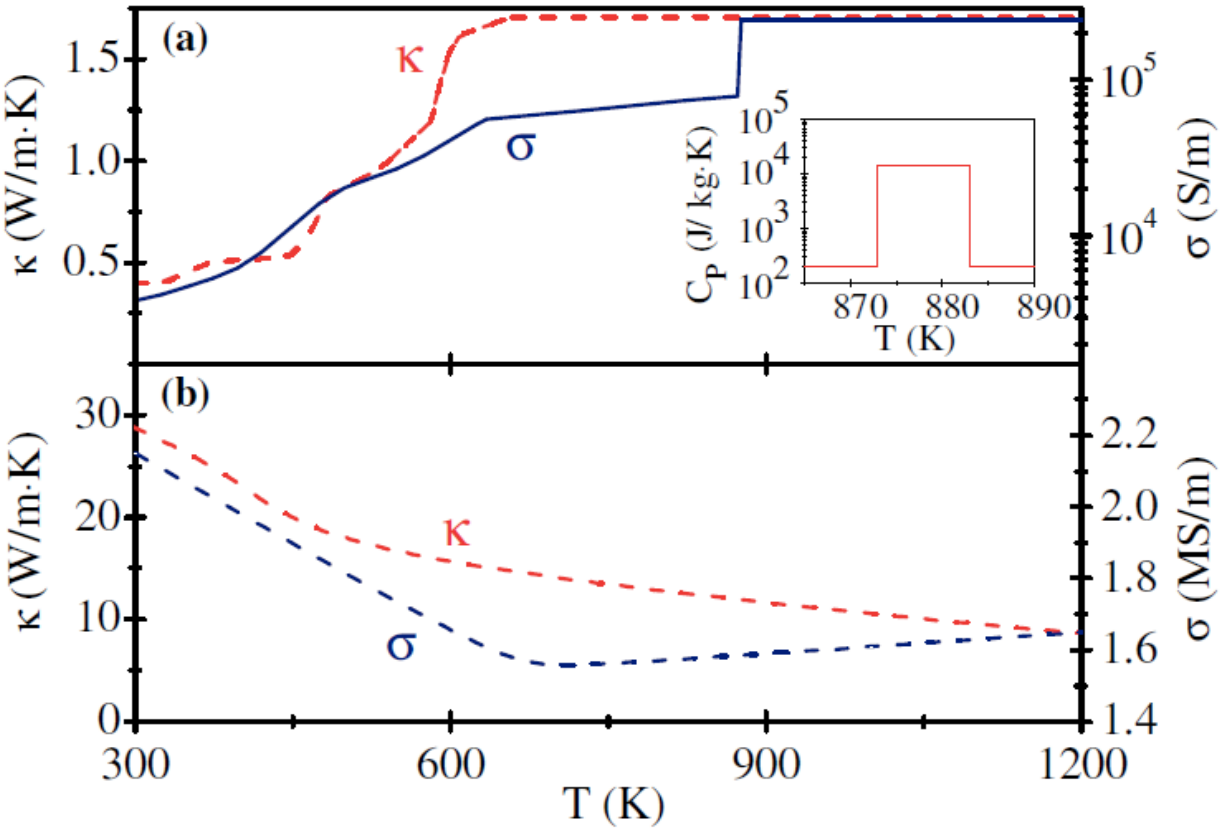

Fig. 3.3 (a) Temperature dependent thermal and electrical conductivity for crystalline (FCC) GST, and (inset) heat capacity incorporating the latent heat of fusion. (b) Temperature dependent thermal and electrical conductivities of TiN.

Unlike many earlier studies in the literature [22], temperature dependent material parameters are used to more accurately simulate device performance. Joule heating in materials with a negative temperature coefficient of resistivity (such as phase change materials) is a process with positive feedback since an increase in current flow causes an increase in temperature, and vice versa, and simulations with only constant value parameters cannot capture this non-linear

behavior of the heating. Figure 3.4 shows a comparison between simulations with our temperature dependent model and with constant-value parameters, where the same volume of GST is melted for each case for the comparison.

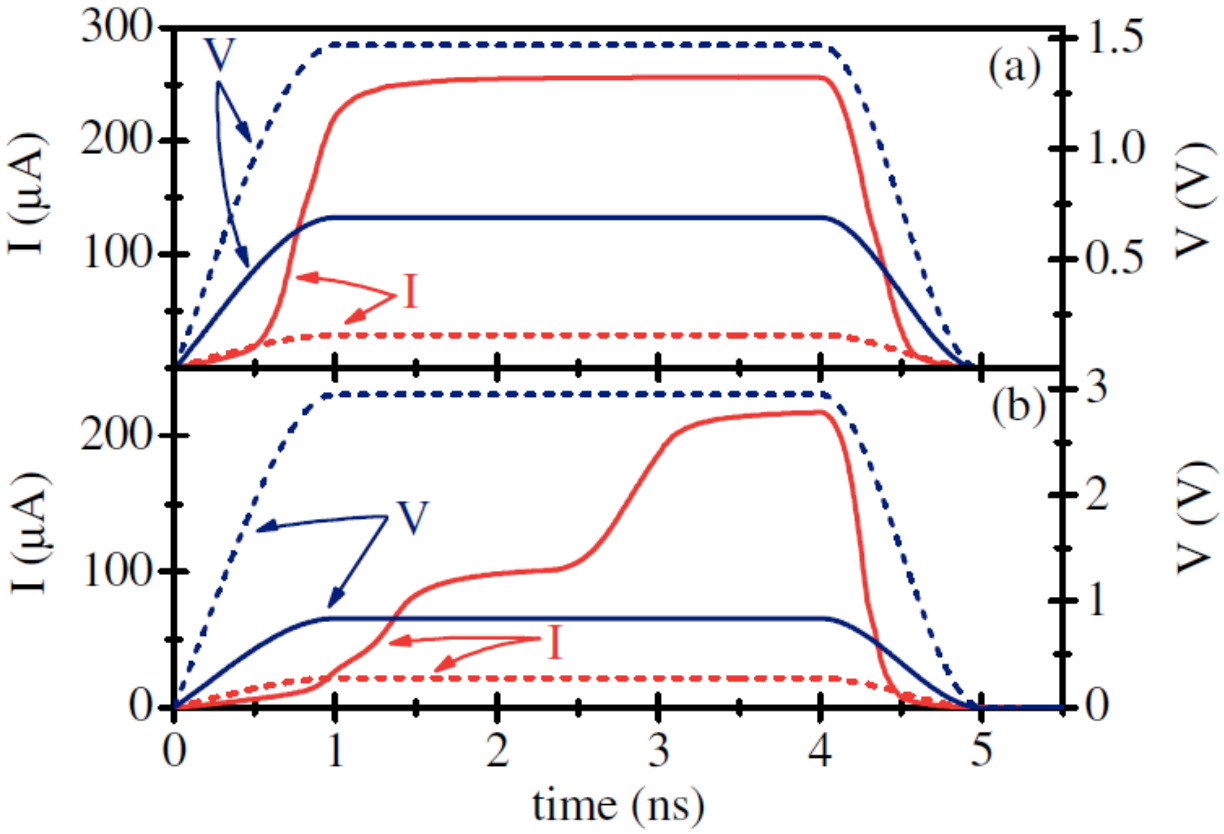

Figure 3.4 I-t and V-t characteristics of reset operation comparing constant value parameters to temperature dependent parameters for reset operation of cells with a 1 kΩ load, 15 nm GST film thickness and (a) 4 nm GST extension length and (b) 16 nm extension length. The same volume of GST is melted for the comparison between the constant-value model(dotted lines) and temperature dependent model (solid line).

The simulations with the constant-value model show constant current throughout the duration of the pulse, and voltage is being significantly overestimated while the current is underestimated. The non-linear heating effects cannot be captured with a model with constant-value material parameters and it is important to use a temperature dependent model to accurately predict device performance.

To predict how variation in geometry affect device performance, we are rearranging the size of mushroom cell in Fig. 3.2(a) with three different geometry.

Now the height of top and bottom electrodes are 100nm with an extension of the Ge2Sb2Te5 (GST) active region with dimensions marked in nm, GST film with diameter 80 nm, height 25 nm and cylindrical TiN pillar, with diameter 8 nm and height 25 nm ± 2.5 nm. Figure 3.5 shows the simulation with three different geometry of planer, recessed and raised mushroom cell. In the recessed cell, 2.5 nm of TiN is replaced with GST so that the active region of GST recedes into the oxide before contacting TiN. The raised cell has an extra 2.5 nm of the TiN channel protruding into the active region of GST.

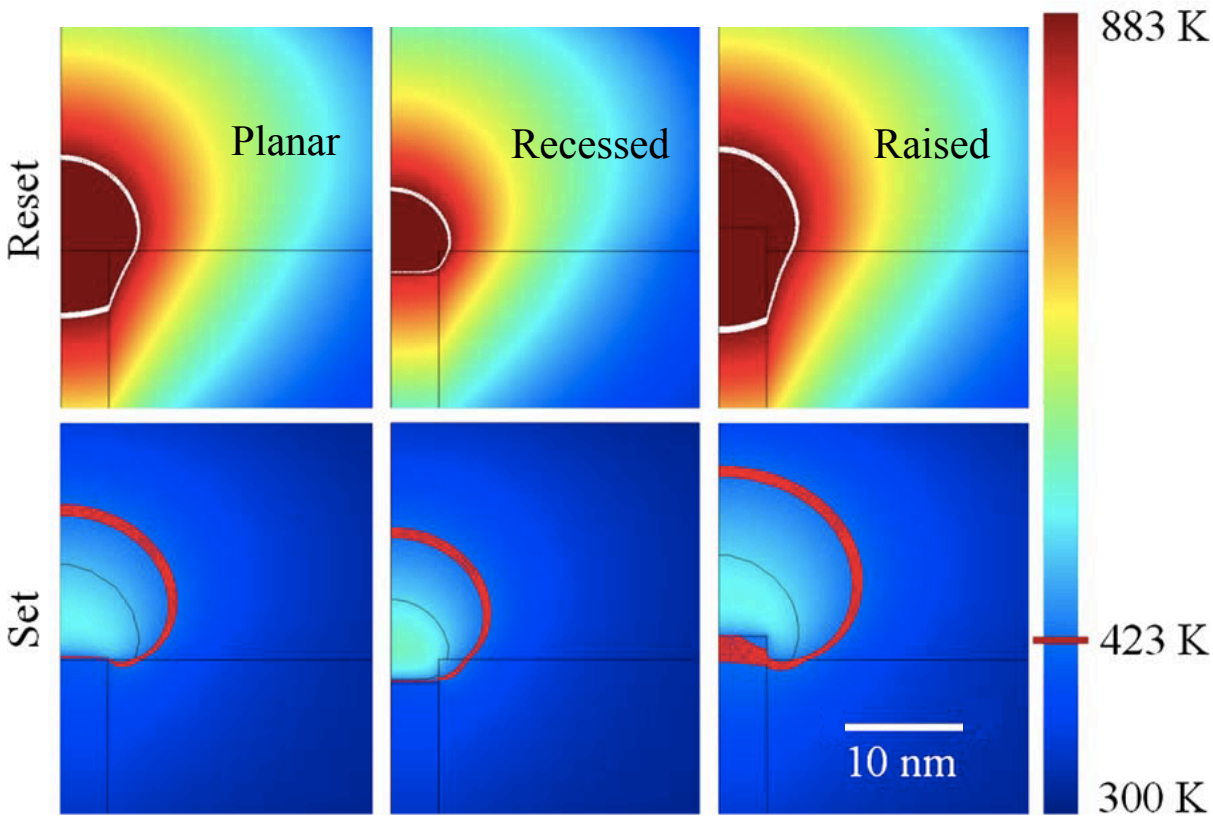

Fig. 3.5 Peak thermal profile of mushroom cells during reset and set pulses. Contour lines are shown to denote the region which has reached the molten temperature (reset) and crystallization temperature (set).

Simulation results indicate that a significant reduction in maximum reset current can be achieved by extending the GST active region into the confined pillar (Figure 3.6). As illustrated in Figure 3.2(b) and 3.5, an extension of the GST active region results in a more favourable thermal profile for heating the entire width of the confined pillar (pillar diameter = 8 nm, in Fig 3.5). The reset current is reduced for a GST extension length

The set pulse voltage is chosen such that the entire amorphous region is over the crystallization temperature (423 K) [13] for approximately 20 ns. The applied voltage pulses for the reset and set operations have total times of 1 and 20 ns, respectively, with 200-ps rise/fall times. The reset pulse voltage is chosen such that at least 2.5 nm of GST is melted in any given direction from the conductive pillar (TiN).

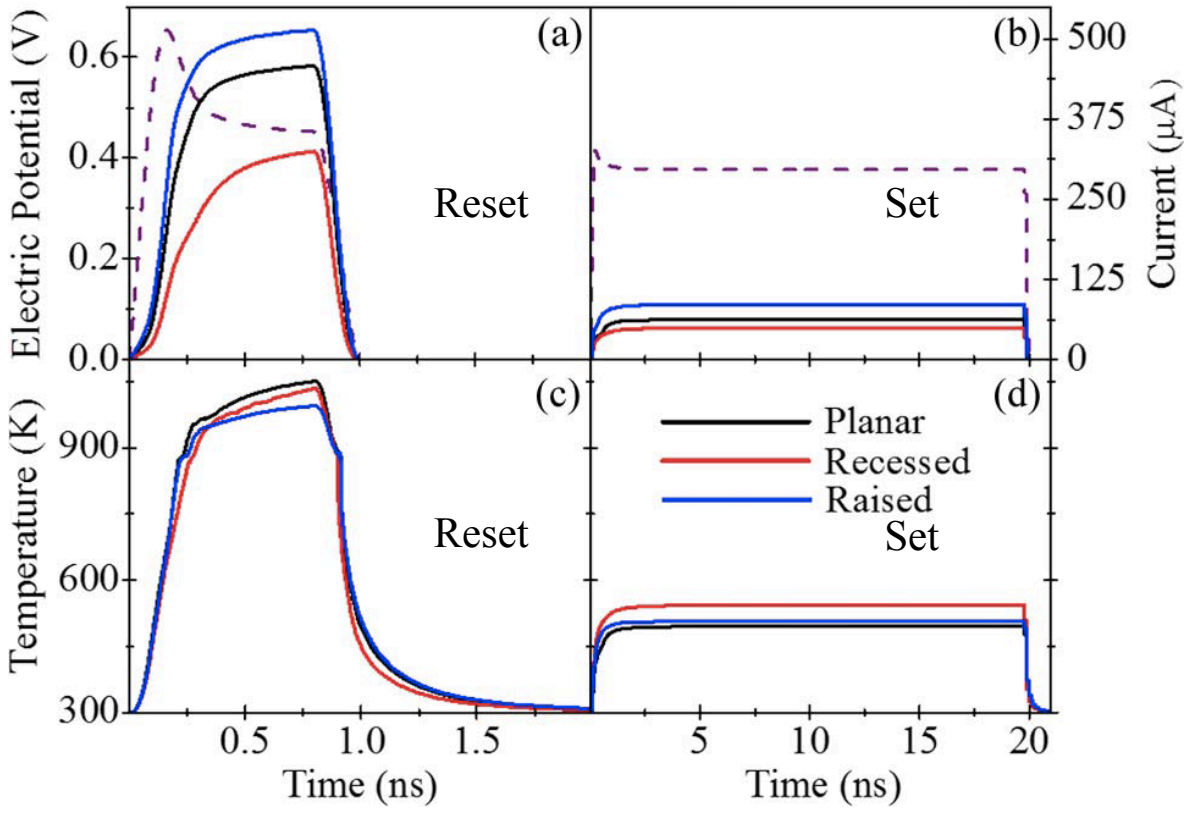

Fig. 3.6 Standard voltage pulse (dashed lines) Current (solid lines) (a) during reset and (b) during set, and (c) Temperature during reset and (d) set operations, measured at the hottest spot in the cell.

3.4 Simulation Results

Table 2

Pulse Type	Pulse time(ns)	Molten Volume(nm^3)	Applied voltage(v)	Vpeak(V)	Ipeak(μA)	Tpeak(K)	Ppeak(μW)
Reset-planer	1	788	0.92	0.653	466	1053	223
Reset-Recessed	1	341	0.81	0.633	298	1038	157
Reset-Raised	1	915	0.97	0.628	534	1004	263
Set-planer	20	-	0.35	0.401	68.3	497	19
Set-recessed	20	-	0.40	0.449	54.8	551	14.6
Set-raised	20	-	0.36	0.391	91.3	512	25.4

Table 2 Reset and Set pulses tile, molten volume, applied voltage, peak voltage, peak current, peak temperature, peak power across the cell.

The confinement due to 2.5-nm recess leads to reduced current and power. The raised cell consumed more power due to increased current while a smaller voltage requirement and set pulse consumed more energy then the reset.

Chapter 4

Summary and Future Work

4.1 Summary

The aim of this project was to design, control and implementation of a phase change memory cell. The cell models includes several equations comprising the Laplace equation and the heat transfer equation. Physical-realistic model provide insight into temporally and spatially resolved kinetics of writing current, device temperature, and phase transition for the required amorphized process. The design incorporates the following innovations:

- Theoretical simulation was performed using the COMSOL Multiphysics (version 5.2) and temperature profiles along the depth direction of the irradiating spoton the GST film were investigated.

- The total conductivity of a-GST is modeled as the combination of the electrical breakdown and temperature dependent components.
- 3-D finite element simulation of joule heating in PCM cell are performed by coupling Heat Transfer and Conductive Media DC Physics Modules.
- Two-dimensional finite element simulations of reset operation in PCM cells are performed to predict how variations in geometry and load resistance affect device performance.
- Simulation results indicate that a significant reduction in maximum reset current can be achieved by extending the GST active region into the confined TiN pillar.

4.1 Future Work

Although many milestones and achievements were reached in this project, this is not a perfect design. The design has the capacity to evolve into a very efficient and there is plenty of room for improvements and added features.

Further research is needed to investigate various phase change materials in Ge-Sb-Te family, theoretically and experimentally in relation to their applications in optical and electrical phase-change data storage to find more reliable and fast threshold switching material for non-volatile phase-change memory cells.

Reference

[1] H. Wong, S. Raoux, S.B. Kim, J. Liang, J. P. Reifenberg, B. Rajendran, M. Asheghi, and K.E. Goodson, “Phase change memory,” Proc. IEEE, vol. 98, no. 12, pp. 2201–2227, Dec. 2010.

[2] D. Ielmini and Y. Zhang, “Analytical model for subthreshold conduction and threshold switching in chalcogenide-based memory devices,” J. Appl. Phys., vol. 102, no. 5, p. 054 517, Sep. 2007.

[3] Sie, C. H. (1969). Memory devices using bistable resistivity in amorphous As−Te−Ge films. Ph.D. dissertation, Iowa State University, Ames, IA.

[4] Pohm, A. V., Sie, C. H., Uttecht, R. R., Kao, V., and Agrawal, O. (1970). Chalcogenide glass bistable resistivity (ovonic) memories. IEEE Transactions on Magnetics, 6: 3.

[5] Wang L., Gong S.D., Yang C.H., Wen J. Towards low energy consumption data storage era using phase-change probe memory with TiN bottom electrode. Nanotechnol. Rev. 2016;5:455– 460. doi: 10.1515/ntrev-2016-0029.

[6] Satoh H., Sugawara K., Tanaka K. Nanoscale phase changes in crystalline Ge2Sb2Te5 films using scanning probe microscopes. Appl. Phys. 2006;99:024306. doi: 10.1063/1.2163010.

[7] Lankhorst, M. H. R., Ketelaars, B. W. S. M. M. & Wolters, R. A.M. Nature Mater. 4, 347–352 (2005).

[8] R. F. Freitas and W. W. Wilcke, "Storage-class memory: The next storage system technology," IBM J. Res. Develop., vol. 52, nos. 4–5, pp. 439–447, 2008.

[9] International Technology Roadmap for Semiconductors (ITRS) Emerging Research Devices, Semi. Ind. Asso., 2013. [Online]

[10] S. Lai and T. Lowrey, "OUM—A 180 nm nonvolatile memory cell element technology for stand alone and embedded applications," in IEDM Tech. Dig., Dec. 2001, pp. 36.5.1–36.5.4.

[11] H. Y. Cheng et al., "A thermally robust phase change memory by engineering the Ge/N concentration in (Ge, N)xSbyTe z phase change material," in IEDM Tech. Dig., Dec. 2012, pp. 31.1. 1–31.1. 4.

[12] H. Y. Cheng et al., "Novel fast-switching and high-data retention phase change memory based on new Ga-Sb-Ge material," in IEDM Tech. Dig., Dec. 2015, pp. 3.5. 1–3.5. 4.

[13] Raoux S et al 2008 IBM J. Res. Dev. 52 465–79

[14] Burr G W, Kim S, Brightsky M, Sebastian A, Lung H-L, Cheng H-Y, Cortes N E S, Wu J Y, Pozidis H and Lam C 2016 IEEE

Journal on Emerging and Selected Topics in Circuits and Systems, issue on‘Emerging Memories— Technology, Architecture & Applications,’ 6 146–62

[15] Burr G W et al 2010 J. Vac. Sci. Technol. B 28 223–62

[16] Bez R and Pirovano A 2004 Mater. Sci. Semicond. Process. 7 349–55

[17] Albert Castell et al.,“Natural convection heat transfer coefficients in phase change material (PCM) modules with external vertical fins”, in ScienceDirect, ELSEVIER, applied thermal engineering 28 (2008) 1676-1686.

[18] Miao Wang, Ming Su; “Thermal-optical readout of multi-level thermal emissivity Ge2Sb2Te5 patterns”, ELSEVER, Materials Letters 257 (2019) 126728.

[19] Lei Wang et al., “Amorphization Optimization of Ge2Sb2Te5 Mediafor Electrical Probe Memory Applications” Nanomaterials (Basel). 2018 Jun; 8(6): 368.

[20] S. Okamine, S. Hirasawa, M. Terao, and Y. Miyauchi, in Opt. Data Storage Top. Meet., edited by D.B.Carlin and D.B. Kay (International Society for Optics and Photonics, 1992), pp. 315–321.

[21] A. Faraclas, G. Bakan, L. Adnane, F. Dirisaglik, N.E. Williams, A. Gokirmak, and H. Silva, IEEE 11 Trans. Electron Devices 61, 372 (2014).

[22] L. Yan, S. Zhi-Tang, L. Yun and F. Song-Lin, "Three-Dimensional Finite Element Analysis of Phase Change Memory Cell with Thin TiO2 Film," Chinese Physics Letters, vol. 27, pp. 038502, 2010.